Separation and Purification Technology 64 (2009) 265–272

Contents lists available at ScienceDirect

Separation and Purification Technology

journal homepage: www.elsevier.com/locate/seppur

Ordered mesoporous silica particles and Si-MCM-41 for the adsorption of acetone: A comparative study

Chinte Hung, Hsunling Bai*, Mani Karthik

Institute of Environmental Engineering, National Chiao Tung University, Hsinchu 300, Taiwan

ARTICLE INFO

Article history:
Received 26 May 2008
Received in revised form 5 October 2008
Accepted 6 October 2008

Keywords:
Molecular sieves
Environmental nanotechnology
Nanomaterials
Volatile organic compounds (VOCs)
Adsorbent and adsorption
Air pollution

ABSTRACT

This study compares the surface properties and the acetone adsorption potentials of mesoporous silica particles (MSPs) and Si-MCM-41. The Si-MCM-41 and MSPs are synthesized, respectively by hydrothermal method and evaporation-induced self-assembly (EISA) method. The results show that the surface area and pore diameter of MSPs are similar to those of Si-MCM-41. But the synthesis of Si-MCM-41 frequently requires longer time and tedious procedure as compared to that of MSPs. The bulk density of MSPs is 3.0–5.0 times higher than that of Si-MCM-41. The mass-based acetone adsorption capacities of these two materials are almost similar. This implies that MSPs have a higher volume-based acetone adsorption capacity than Si-MCM-41 so that less space is required for volatile organic compounds (VOCs) adsorption using MSPs as the adsorbent. The pressure drops of both powder and pellet forms of MSPs are also smaller than those of Si-MCM-41 for adsorbing the same amount of acetone. In addition, as compared to commercial H-ZSM-5 zeolite, both MSPs and Si-MCM-41 reveal better performances on the regeneration ability. As a result, both MSPs and Si-MCM-41 show high adsorption/desorption potential but the MSPs are better as novel adsorbents in terms of overall engineering consideration.

1. Introduction

Volatile organic compounds (VOCs) are major air pollutants which need to be controlled due to increasingly stringent environmental regulations. Numerous technologies such as adsorption, incineration, thermal oxidation and catalytic reduction have been developed and applied world-wide for the removal of VOCs [1]. Among the VOCs removal processes, the adsorption process is widely applied because of the system flexibility, low cost as well as low energy consumption. And ZSM-5 zeolite-based rotors have replaced the activated carbon adsorbers in the semi-conductor and opto-electronic industries as viable VOCs concentrators [2] because of their unique properties such as hydrophobicity, thermal stability as well as high regenerative ability.

Recently the highly ordered mesoporous silica molecular sieves have received much attention because of their potential applications in the fields of adsorption, separation, catalysis, and environmental pollution control [3,4]. Mobil researchers [5] reported the first family of highly ordered mesoporous molecular sieves (M41S) by using long-chain cationic surfactant as the template or pore forming agent during the hydrothermal sol–gel synthesis. Since then, numerous mesoporous silica and other metal oxides with narrowly distributed mesopore diameters of 2–50 nm have been synthesized through various synthetic routes for obtaining materials in different chemical compositions and pore structures. And their potential applications as adsorbents have been extensively studied [6–14].

Zhao et al. [14] obtained the VOCs adsorption isotherms of MCM-41, zeolites and activated carbon. The results showed that by comparing with the performance of activated carbon, the adsorption capacity of MCM-41 is lower for VOCs with low vapor pressures but higher for VOCs with high vapor pressures due to the type IV isotherm characteristic of MCM-41. Besides, desorption of VOCs from MCM-41 could be achieved at lower temperatures (50–60 °C), while this had to be conducted at higher temperatures (100–120 °C) for zeolites and activated carbons.

Although several synthetic pathways are well known to prepare the mesoporous materials of MCM-41, most of the synthetic strategies are tedious and time-consumed with several days of operation time. A new aerosol-processing route of evaporation-induced self-assembly (EISA) method for synthesizing ordered mesoporous silica particles (MSPs) has been developed by Lu et al. [15]. The advantage of the EISA method lies in that it can continuously produce MSPs in a very short processing time of a few seconds plus a few hours of calcination.

The EISA method combines the simplicity of sol–gel process and aerosol-assisted process with the efficiency of surfactant self-

* Corresponding author. Tel.: +886 3 5731868; fax: +886 3 5725958.
E-mail address: hlbai@mail.nctu.edu.tw (H. Bai).

1383-5866/$ – see front matter.
doi:10.1016/j.seppur.2008.10.020

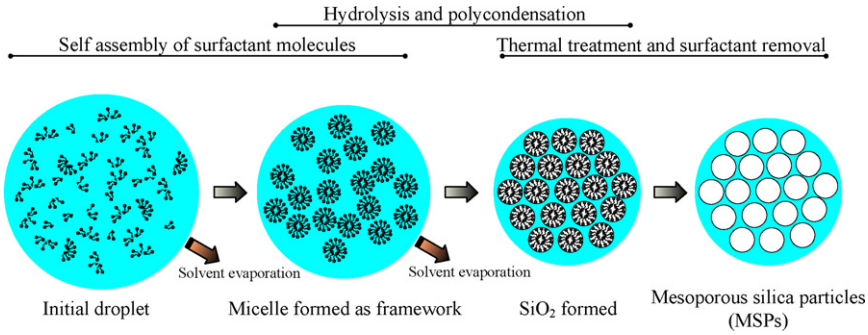

Fig. 1. The formation mechanism of MSPs.

assembly mechanism. Fig. 1 illustrates the possible formation mechanism [16] of MSPs. The reagents are firstly atomized into aerosol droplets and the surfactant molecules start to be self-assembled as the solvent of droplets evaporates. Meanwhile, the inorganic condensation is achieved via sol–gel process. Finally, the mesoporous silica structured particles are obtained after the removal of surfactant molecules.

Our research group has been the first to use MSPs as alternative adsorbents for VOCs emission control due to their hydrophobic and easy recovery properties [17–19]. However, to the authors' knowledge, there has been no report available on comparing the Si-MCM-41-based mesoporous materials and the MSPs for the VOCs adsorption. In this study, both Si-MCM-41 and MSPs are synthesized, respectively by the hydrothermal method and the EISA method. The structure, morphology, BET characteristics, pressure drop, bulk density, and the acetone adsorption capacity of these two mesoporous silica adsorbents are compared. The performances of these two novel mesoporous adsorbents are also compared with that of the commercial silica-based adsorbent of H-ZSM-5 zeolite to understand their industrial applicability.

2. Experimental

2.1. Preparation of MSPs

Mesoporous silica particles were continuously synthesized by the EISA process. Tetraethoxysilane (TEOS) and cetyltrimethyl ammonium bromide (CTAB) were employed as the silica source and the structure-directing template, respectively. Molar compositions of the gel mixture were SiO_2:0.18 CTAB:10 ethanol:40 H_2O:0.008 HCl. The precursor mixture was nebulized by an ultrasonic atomizer as carried by high-pressure air. The reactor was consisted of two heating zones, the first zone was operated at a temperature of 150 °C and the second zone was operated at a temperature of 550 °C. The total synthesis time of this continuous flow process was approximately 4–6 s to generate the MSPs adsorbent. The synthesized adsorbent was collected downstream of the reactor with a high efficiency filter and then placed in a muffle furnace for 4 h at a calcination temperature of 550 °C to remove the organic structure-directing template. Detailed description of the synthesized procedure is referred to Hung and Bai [19].

2.2. Preparation of Si-MCM-41

Hexagonal mesoporous Si-MCM-41 material was synthesized by the hydrothermal method which is one of the most common techniques for preparing MCM-41 materials. Molar compositions of the gel mixture were SiO_2:0.2 CTAB:0.89 H_2SO_4:120 H_2O. In a typical synthesis procedure, 21.2 g of sodium metasilicate nanohydrate was dissolved in 80 ml DI water and the resulting solution was stirred vigorously for 30 min. Then approximately 40 ml of 4N H_2SO_4 was added to the above mixture to bring down the pH to 10.5 with constant stirring to form a gel. After stirring, 7.28 g of CTAB (dissolved in 25 ml of DI water) was added slowly into the above mixture and the combined mixture was stirred for three additional hours. The resulting gel mixture was transferred into a Teflon-coated autoclave and kept in an oven at 145 °C for 36 h. After cooling to the room temperature, the resultant solid was recovered by filtration, washed with DI water and dried in an oven at 110 °C for 8 h. Finally, the organic template was removed by calcination using a muffle furnace in air at 550 °C for 10 h. The total synthesis time for the Si-MCM-41 by hydrothermal method was about 60 h.

2.3. Characterization of the adsorbents

Nitrogen adsorption and desorption isotherms of the synthesized materials were measured at −196 °C using a surface area and pore diameter distribution analyzer (Micromertitics, ASAP 2020, USA). Prior to the adsorption–desorption measurements, the samples were degassed at 350 °C for 6 h under vacuum pressure of 10^{-6} mbar. The powder X-ray diffraction patterns (XRD) of MSPs and Si-MCM-41 materials were obtained using a Rigaku D/MAX-B diffractometer equipped with a Cu Kα radiation at λ = 1.54 Å. The diffractograms of the MSPs and Si-MCM-41 were recorded in the 2θ range of 2–10° with steps of 0.6° and a count time of 60 s at each point. The surface morphology of MSPs and Si-MCM-41 was characterized using transmission electron microscopy (TEM, Hitachi H7100 and JEOL JEM 1210, Japan). The TEM samples (5–10 mg) were ultrasonicated in ethanol solution and the resulting suspensions were dispersed on carbon film supported 200 mesh copper grids. The samples were then measured and observed by TEM at an acceleration voltage of 200 kV.

2.4. Acetone adsorption by TGA

A thermo-gravimetric analyzer (TGA, Netzsch TG 209 F1, German) was used to measure the mass changes of adsorbents during the adsorption and desorption processes. Adsorbents (10 mg) were loaded on the TGA sample holder and purged with nitrogen at a temperature of 200 °C for 1 h before acetone adsorption. The inlet flow rate was 60 cm^3/min during each adsorption experiment. Except for studying the effects of acetone inlet concentration and temperature on the acetone adsorption, the base line test conditions were at an acetone inlet concentration of 8700 ± 100 ppmv and isothermal temperature of 45 °C. The acetone adsorption was carried out for at least 1 h until no mass change was observed. And the acetone desorption was conducted by purging with clean air under 200 °C for 24 h.

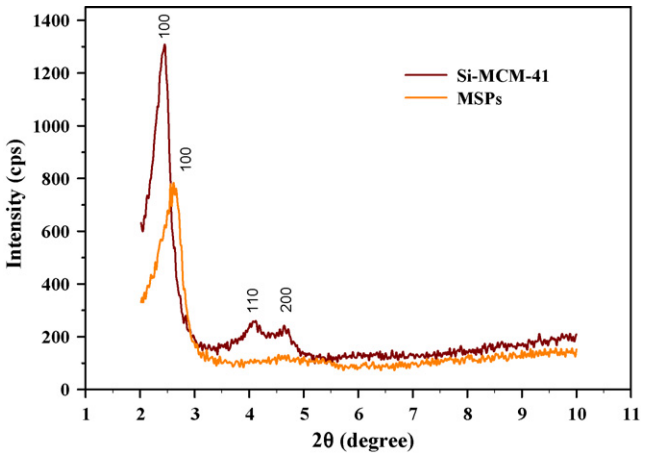

Fig. 2. XRD patterns of MSPs and Si-MCM-41 adsorbents.

3. Results and discussion

3.1. Characterization of the adsorbents

3.1.1. XRD analysis

Powder low-angle XRD patterns of calcined MSPs and Si-MCM-41 are depicted in Fig. 2. They clearly indicated characteristic low-angle peaks of mesoporous materials. The XRD pattern of Si-MCM-41 exhibited a well ordered structure and the peaks are indexed on a hexagonal lattice corresponding to (1 0 0), (1 1 0), and (2 0 0) reflections [5]. On the other hand, the XRD pattern of MSPs revealed only one reflection peak (1 0 0) which was the characteristic evidence of hexagonal mesoporous structure of spherical particles [20,21]. The absence of (1 1 0) and (2 0 0) reflection peaks for MSPs indicated that it has a different pore structure from that of Si-MCM-41 due to the smaller size of periodic mesoporous areas. It was also observed that the intensity of (1 0 0) reflection is smaller for MSPs as compared to that of the Si-MCM-41. Besides, the (1 0 0) reflection peak of MSPs shifted to a higher value of reflection angle which revealed the decrease in periodic distance between pores.

3.1.2. BET analysis

The nitrogen adsorption–desorption isotherms of calcined MSPs and Si-MCM-41 materials are shown in Fig. 3. Both samples exhibited isotherms of type IV based on the IUPAC classification.

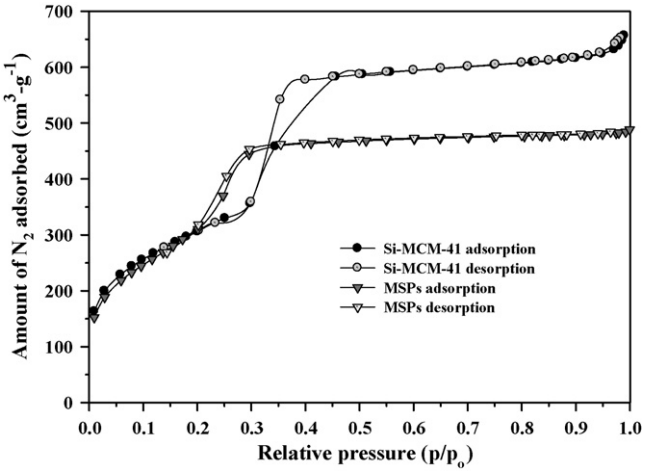

Fig. 3. Nitrogen adsorption–desorption isotherms of MSPs and Si-MCM-41 adsorbents.

Table 1
Physical properties characterized by XRD and BET analysis.

Materials	S_{BET} [a] (m^2/g)	V_P [b] (cm^3/g)	d_{BJH} [c] (nm)	d_{100} [d] (nm)	a_0 [e] (nm)
MSP	1153	0.89	2.4	3.4	3.9
Si-MCM-41	1115	0.97	2.7	3.9	4.5

[a] BET specific surface area.
[b] Pore volume.
[c] Pore diameter calculated by BJH method.
[d] d-spacing.
[e] Unit cell ($a_0 = 2d_{100}/\sqrt{3}$).

The sharp increases in the quantity of nitrogen adsorption were observed at relative pressures (p/p_o) of 0.2–0.3 for MSPs and 0.3–0.4 for Si-MCM-41, which are the evidence of capillary condensation of nitrogen within the primary mesopores. And both materials exhibited reversible feature of isotherms with hysteresis loops between adsorption and desorption processes. The isotherm curves of these two materials were almost the same at p/p_o = 0–0.2 before capillary condensation occurs. This region corresponded to monomolecular layer adsorption of nitrogen molecules (Langmuir adsorption). The capillary condensation of nitrogen molecules within the mesopores was shifted to a lower value of p/p_o for MSPs than the Si-MCM-41.

The physical properties such as BET specific surface area, specific pore volume and the average pore diameter (BJH) of the mesoporous materials are summarized in Table 1. The MSPs had a slightly higher specific surface area of 1153 m^2/g than that of Si-MCM-41, 1115 m^2/g. On the other hand, the average pore diameter and specific pore volume of Si-MCM-41 was slightly higher than that of mesoporous silica particles.

3.1.3. TEM analysis

The TEM images of MSPs and Si-MCM-41 are shown in Fig. 4. The TEM images of MSPs clearly exhibited a well ordered mesoporous spherical particles, while the morphology of Si-MCM-41 showed a well ordered long-range-hexagonal array of mesoporous structure with uniform pore diameter. However, the pore channels of MSPs were constructed and arranged in two-dimensional orientation while those of Si-MCM-41 were in one-dimensional orientation.

The arrangement and growth orientation of mesoporous channels of MSPs and Si-MCM-41 based on the TEM images are sketched in Fig. 5. The pore channels of MSPs were bended as compared to the straight channels of Si-MCM-41. The formation of bending channels was due to that the pore channels had to fit into the spherical shape of MSPs during periods of the self-assembly stage of surfactant molecules and the formation of porous framework.

3.2. Bulk density and VOCs adsorption

3.2.1. Bulk density

The bulk densities of adsorbents are expressed in terms of mass per packed volume of adsorbents which include the space among MSPs or Si-MCM-41 adsorbent particles upon packing. Measurements of the bulk density for the adsorbents are referring to ASTM D6683-01 [22]. The bulk densities after various standard screen meshes are listed in Table 2. The #50 mesh corresponds to screened particle size of >294 μm while the #100 mesh corresponds to screened particle size of <149 μm. It can be seen that the smaller the Si-MCM-41 adsorbent powder was, the less bulk density it possessed. However, the bulk densities of MSPs were not a function of particle size. The bulk densities of MSPs powders and pellets were 3–5 times higher than those of Si-MCM-4. Since the pore diameter and surface area of these two adsorbents were similar, the higher bulk density of MSPs is attributed to its spherical

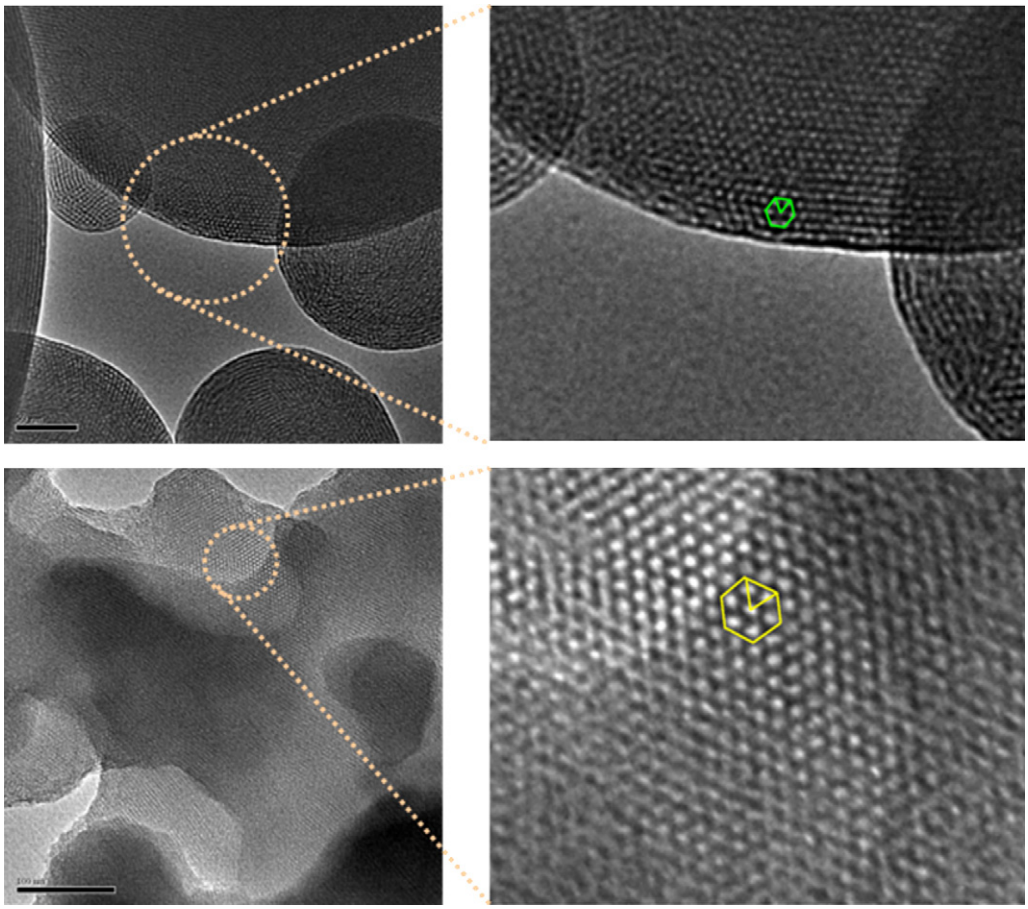

Fig. 4. Transmission electronic microscope (TEM) images of MSPs (left-top) and Si-MCM-41 (left-bottom). The scale bar on the top image is 50 nm and at the bottom is 100 nm. Images on the right hand side are the enlargements of the TEM images.

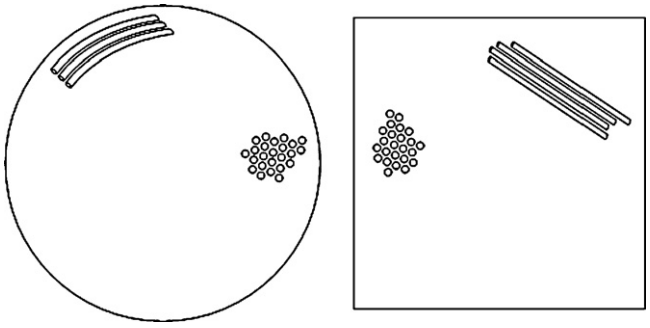

Fig. 5. Schemes of opening pores and channels of MSPs (left) and Si-MCM-41 (right).

shape which could be packed more densely than the Si-MCM-41 material with amorphous shapes.

The higher bulk density of the MSPs indicates that as compared to the Si-MCM-41 material, the adsorber volume of VOCs can be significantly reduced using MSPs as an adsorbent if their mass basis adsorption capacities (mg VOCs/g adsorbent) are about the same. In addition to be applied for the end-of-pipe VOCs adsorption purposes, this advantage may also enable the MSPs to be applied as an alternative adsorbent during VOCs sampling and analysis [23].

3.2.2. Adsorption capacity and regeneration ability

To understand the potential application of these two mesoporous adsorbents, adsorption tests were also performed on a commercial silica-based adsorbent, the H-ZSM-5 zeolite. The ZSM-5-based zeolite materials are widely used as the adsorbents in temperature swing adsorbers (zeolite concentrators) for continuous VOCs adsorption and desorption [24]. The NH_4-form of ZSM-5 zeolite (Si/Al = 50) was purchased from Zeolyst Pvt. Ltd. Prior to the adsorption experiments, the NH_4-form of ZSM-5 zeolite was converted into H-form of ZSM-5 by calcination at 550 °C for 6 h.

Fig. 6a shows results on the comparison of equilibrium acetone adsorption capacities of MSPs, Si-MCM-41, and H-ZSM-5 zeolite on a mass basis (mg/g). The acetone adsorption capacities of MSPs

Table 2
Bulk densities of MSPs and Si-MCM-41 powders and pellets (unit: g/cm^3).

Particle mesh (particle size)	Pellet		Powder					
	10–20 mesh (830–1700 μm)		50 mesh (>294 μm)		50–100 mesh (149–294 μm)		100 mesh (<149 μm)	
	Average	S.D.	Average	S.D.	Average	S.D.	Average	S.D.
MCM-41	0.162	0.005	0.096	0.001	0.095	0.003	0.068	0.01
MSP	0.501	0.009	0.359	0.009	0.372	0.002	0.355	0.002
H-ZSM-5	–	–	–	–	–	–	0.475	0.011

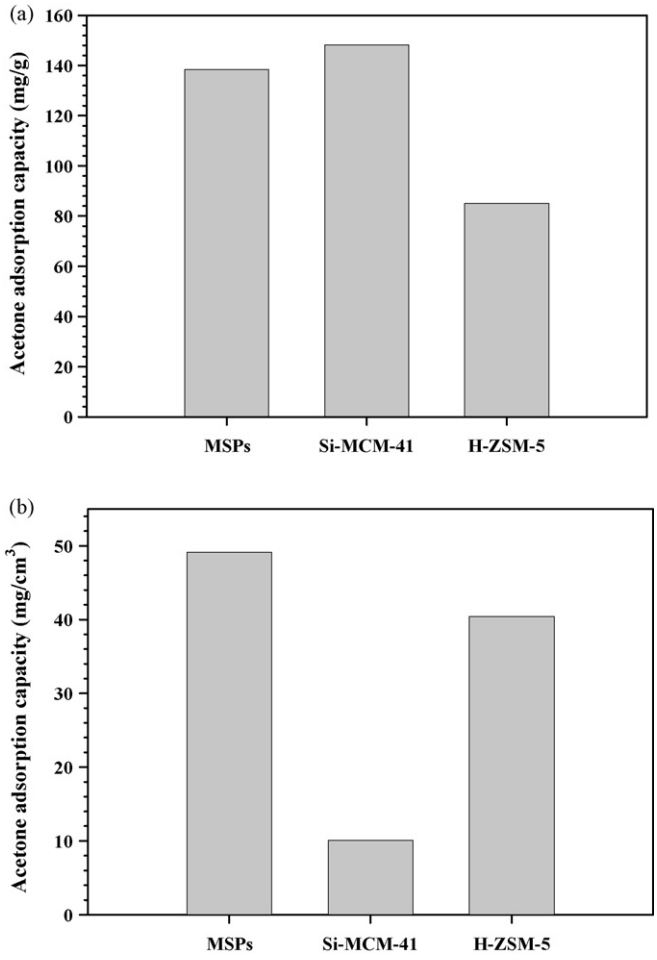

Fig. 6. (a) Mass basis comparison on the equilibrium acetone adsorption capacities of MSPs, Si-MCM-41 and H-ZSM-5. The adsorbent powders were <100 mesh in size. (b) Volume basis comparison on the equilibrium acetone adsorption capacities of MSPs, Si-MCM-41 and H-ZSM-5. The adsorbent powders were <100 mesh in size.

and Si-MCM-41 (both at <100 mesh size) for an acetone inlet concentration of 8700 ppmv at 45 °C were 138 mg/g and 148 mg/g, respectively, as tested on the freshly made adsorbents. The MSPs and Si-MCM-41 had similar adsorption capacities. And they showed much higher adsorption capacities as compared to that of microporous H-ZSM-5 zeolite (adsorption capacity of 85 mg/g).

Fig. 6b compares the equilibrium acetone adsorption capacity of MSPs, Si-MCM-41, and H-ZSM-5 zeolite on a volume basis (mg/cm^3). For practical engineering application, the adsorber volume is highly concerned due to space limitation. The result reveals that the acetone adsorption capacity of MSPs is 49 mg/cm^3, which is almost five times of that of the Si-MCM-41, 10 mg/cm^3. For the case of H-ZSM-5 zeolite, the volume basis acetone adsorption capacity is 40 mg/cm^3, which is less than that of MSPs but much higher than that of Si-MCM-41. This provides a high advantage for practical adsorption application using MSPs since it can reduce the adsorber volume of VOCs adsorption.

Fig. 7 shows the adsorption–desorption performance of MSPs, Si-MCM-41 and H-ZSM-5 zeolite in terms of adsorption index (%). The adsorption index (%) was calculated based on the ratio of adsorption capacity of the regenerated adsorbent to the fresh one, thus 100% of adsorption index indicates that the adsorbent is not deteriorated at all.

It can be seen from Fig. 7 that both MSPs and Si-MCM-41 adsorbents showed almost no deterioration after regeneration. The

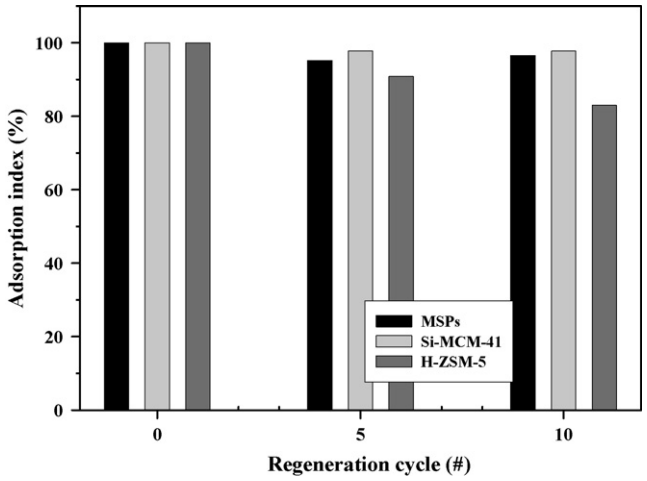

Fig. 7. Comparison results on the regeneration ability of MSPs, Si-MCM-41 and H-ZSM-5 adsorbents. The sizes of adsorbent powders were <100 mesh.

adsorption indexes of MSPs after 5 and 10 regeneration cycles were 95.2% and 96.5%, respectively, while the adsorption indexes for Si-MCM-41 adsorbent were 97.7% and 97.7%, respectively. On the other hand, the H-ZSM-5 zeolite had a significant deterioration after 10 regeneration cycles so that its adsorption index decreased to only 83.0%. The high values of adsorption index for MSPs and Si-MCM-41 are due to the pure silica framework without aluminum species as compared to the H-ZSM-5 zeolite (Si/Al ratio = 50). The presence of aluminum species would catalyze the adsorbed acetone into coke during the regenerating process and lead to the deterioration of adsorbents [17].

3.2.3. Adsorption isotherms and temperature effect

Acetone adsorption isotherms for MSP and Si-MCM-41 adsorbents are examined by fitting the experimental data to Langmuir and Freundlich isotherm models:

$$\text{Langmuir}: \ q_e = \frac{q_m K_a C_e}{1 + K_a C_e} \quad (1)$$

$$\text{Freundlich}: \ q_e = K_F {C_e}^{1/n_f} \quad (2)$$

where C_e (ppmv) and q_e (mg/g) are the gas phase concentration and solid phase adsorption quantity of acetone at equilibrium, respectively; K_a is the Langmuir isotherm constant (1/ppm); q_m (mg/g) is the single layer acetone adsorption capacity; K_F is the Freundlich constant; n_f is the heterogeneity factor. The Langmuir and Freundlich adsorption isotherm parameters for the adsorption of acetone vapors on the MSPs and Si-MCM-41 adsorbents are listed in Table 3. The values of $n_f > 1$ in Freundlich isotherm reflected that acetone vapors were favorably adsorbed on the MSPs and Si-MCM-41 adsorbents.

Fig. 8a and b illustrates the Langmuir and Freundlich adsorption isotherms, respectively, for the adsorption of acetone on MSPs

Table 3
Summary of the Langmuir and Freundlich isotherm constants.

Isotherm		Parameters	Adsorbent	
			MSPs	Si-MCM-41
Langmuir isotherm	$q_e = \frac{q_m K_a C_e}{1+K_a C_e}$	q_m	141.1	157.6
		K_a	0.0021	0.0009
		R^2	0.996	0.990
Freundlich isotherm	$q_e = K_F {C_e}^{1/n_f}$	K_F	47.38	20.17
		n_f	8.62	4.62
		R^2	0.999	0.996

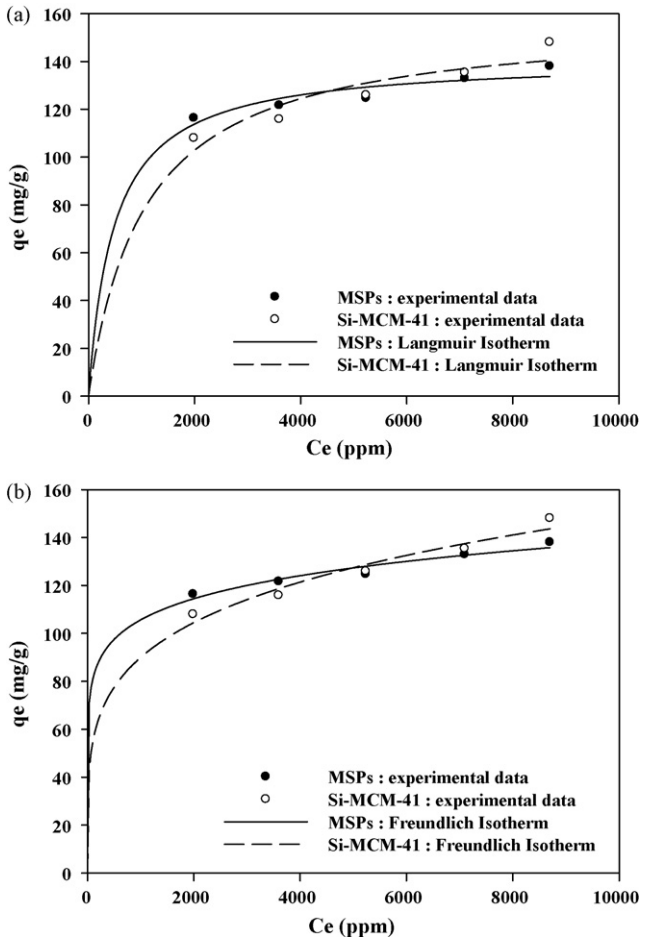

Fig. 8. (a) Langmuir adsorption isotherm for MSPs and Si-MCM-41 adsorbents. The sizes of adsorbent powders were <100 mesh. (b) Freundlich adsorption isotherm for MSPs and Si-MCM-41 adsorbents. The sizes of adsorbent powders were <100 mesh.

and Si-MCM-41 adsorbents. The fitted results of both Langmuir and Freundlich isotherms were in good fitting relationship over the studied concentration range of 2000–8700 ppmv. And the Freundlich adsorption isotherm model was better (with correlation coefficient R^2 of 0.996–0.999) than the Langmuir isotherm (R^2 of 0.990–0.996) to describe acetone adsorption behaviors on both MSP and Si-MCM-41 adsorbents.

The temperature effects on the equilibrium acetone adsorption capacities of MSP and Si-MCM-41 adsorbents were performed in the range of 25–105 °C and the results are shown in Fig. 9. One can see that the adsorption capacity of MSPs was slightly less than that of the Si-MCM-41 for all tested temperature, but the decreasing trend in adsorption capacity with increasing temperature was very similar between these two adsorbents. At an adsorption temperature of 25 °C the adsorption capacities of these two adsorbents were around 190 mg/g and they decreased to the values of around 50 mg/g at 105 °C.

3.3. Pressure drop measurement

The pressure drop of an adsorbent is another important issue that needs to be considered for field application. In this study, the pressure drops were measured by columns packed with either powder (50–100 mesh) or pellet (10–20 mesh) types of adsorbents. The pellet type adsorbents can be used for air pollution control purpose of VOCs presented in indoor or waste gas stream (i.e. end-of-pipe

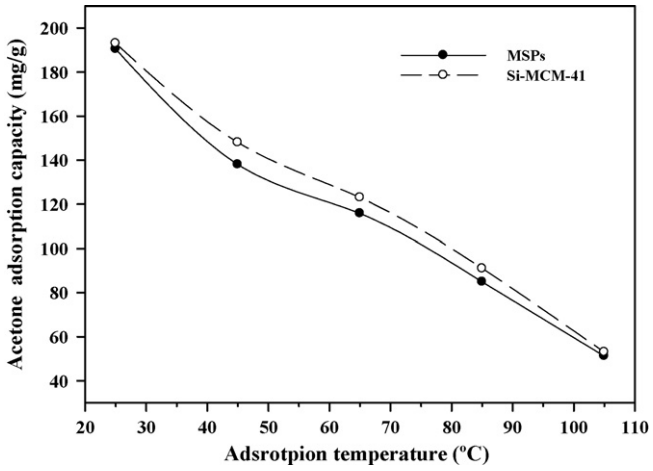

Fig. 9. Temperature effect on the equilibrium acetone adsorption capacities of MSPs and Si-MCM-41 adsorbents. The sizes of adsorbent powders were <100 mesh.

application), while the powder type adsorbent can be packed in the column for atmospheric VOCs sampling or analysis. Clean compressed air was used as the test stream that passed through the column at different values of superficial velocity (i.e. the empty bed velocity). It is noted that although the pressure drops for commercial adsorbents are usually expressed as ΔP/packed height, but because MSPs and Si-MCM-41 have similar adsorption capacity on a mass basis, so in this study the pressure drop is expressed in ΔP/g in order to explore the total pressure drop encountered to adsorb similar quantity of VOCs adsorbent.

Values of pressure drop for powder types of MSPs and Si-MCM-41 adsorbents as a function of superficial velocity are depicted in Fig. 10a. It showed significant different values of pressure drop between Si-MCM-41 and MSPs adsorbents. The pressure drop of Si-MCM-41 was increased drastically with increasing the superficial velocity so that the pressure drop measurement could not be continued at superficial velocity of over 0.1 m/s. On the other hand, the pressure drop of MSPs powder adsorbent was not only lower than that of the Si-MCM-41, but also increased at a slower rate as the superficial velocity was increased.

Fig. 10b shows the pressure drops of pellet types Si-MCM-41 and MSPs adsorbents. One can observe that the pressure drops were increased with increasing the superficial velocity and the overall pressure drops of Si-MCM-41 adsorbents were larger than that of MSPs adsorbents except at superficial velocity of less than 1.0 m/s where the pressure drops of both materials were about the same.

The cause in significant deviation in the pressure drop between powder forms of MSPs and Si-MCM-41 can be explained by the Ergun equation [25]:

$$\Delta P = L\left[E_1\frac{\mu U_g}{d_P^2}\frac{(1-\varepsilon)^2}{\varepsilon^3} + E_2\frac{\rho U_g^2}{d_P}\frac{(1-\varepsilon)}{\varepsilon^3}\right] \quad (3)$$

where U_g is the fluid velocity; ΔP is the pressure drop; L is the length of the porous medium; μ and ρ are the fluid viscosity and fluid density, respectively; E_1 and E_2 are Ergun constants; ε is the inter-particle void fraction; d_P is the mean particle diameter of the granular medium. The first term on the right side of the Ergun equation corresponds to the Blake-Kozeny laminar flow conditions and under such conditions the second term on the right hand side can be ignored. As a result, the pressure drop is linearly correlated to the fluid velocity under the Blake-Kozeny laminar flow conditions as observed from Fig. 10a and b that the pressure drop is linearly correlated to the fluid velocity. This indicated that only the first term of Ergun equation needs to be considered in this study, thus

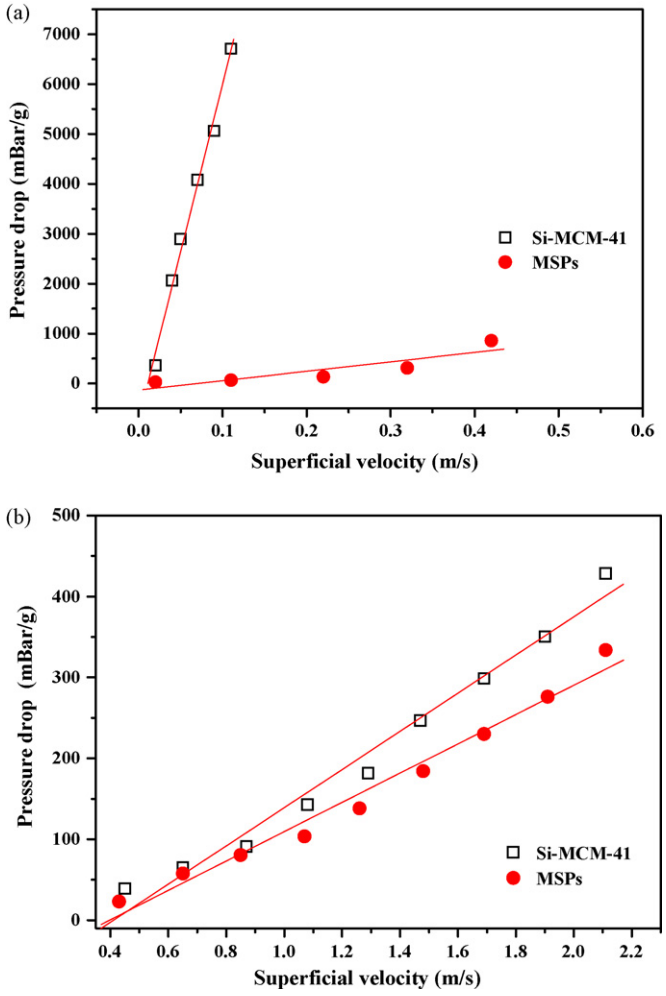

Fig. 10. (a) Pressure drops for powder types (50–100 mesh) of MSPs and Si-MCM-41 adsorbents. (b) Pressure drops for pellet types (10–20 mesh) of MSPs and Si-MCM-41 adsorbents.

the Ergun equation is reduced to the form:

$$\Delta P = L\left[E_1 \frac{\mu U_g}{d_P^2} \frac{(1-\varepsilon)^2}{\varepsilon^3}\right] \quad (4)$$

Because the pressure drop tests of MSPs and Si-MCM-41 were done at a similar particle size range of 149–294 μm (50–100 mesh) under the same flow condition, thus the pressure drop in Eq. (4) depends on the inter-particle void fraction (ε) and the length of the porous medium (L) in this study. The void fraction (or porosity) of the powder form of Si-MCM-41 should be initially higher than that of the MSP. However, the powder form of Si-MCM-41 is in irregular, flakes-like shapes and was loosely packed as compared to the spherical shape MSP powder. As the gas flowing into the adsorber, the Si-MCM-41 powders were significantly compressed and became very dense, which resulted in a very high-pressure drop due to rapid decrease in the void fraction. On the other hand for the pellet types of MSPs and Si-MCM-41, because both of them had been compressed before pressure drop tests so their pressure drops did not show a significant difference as observed for the powder forms.

4. Conclusions

Mesoporous silica particles are very competitive as a VOCs adsorbent not only to the commercialized HZSM-5 zeolite but also to the Si-MCM-41. The MSPs can be produced by a time-saving synthesized process and it has a better adsorption performance. Both of its mass-based acetone adsorption capacity and regeneration ability are similar to those of Si-MCM-41 adsorbent, and they are much higher than those of H-ZSM-5 zeolite. The higher bulk density of MSPs adsorbents leads to a higher volume-based adsorption capacity than that of the Si-MCM-41. To adsorb the same quantity of acetone, the pressure drop of MSPs is also lower than that of Si-MCM-41. As a result, less space and less energy are required when MSPs are utilized as an adsorbent.

Acknowledgement

The authors would like to thank the National Science Council of Taiwan for its financial supports under contract numbers NSC94-2211-E-009-046, NSC95-2221-E-009-192 and NSC96-2221-E-009-045.

References

[1] F.K. Khan, A.K. Ghosal, Removal of volatile organic compounds from polluted air, Journal of Loss Prevention in the Process Industries 13 (2000) 527–545.
[2] Y.C. Lin, H. Bai, C.L. Chang, Adsorption of acetone on hexagonal nanostructured zeolite particles, Journal of Environmental Engineering and Management 14 (2) (2004) 99–106.
[3] S. Kawi, M. Te, MCM-48 supported chromium catalyst for trichloroethylene oxidation, Catalysis Today 44 (1998) 101–109.
[4] Q.H. Xia, K. Hidajat, S. Kawi, Adsorption and catalytic combustion of aromatics on platinum-supported MCM-41 materials, Catalysis Today 68 (2001) 255–262.
[5] J.S. Beck, J.C. Vartuli, W.J. Roth, M.E. Leonowicz, C.T. Kresge, K.D.C. Schmitt, T.W. Chu, D.H. Olson, E.W. Sheppard, S.B. Higgins, J.L. Schlenker, A new family of mesoporous molecular sieves prepared with liquid crystal templates, Journal of American Chemical Society 114 (1992) 10834–10843.
[6] X.S. Zhao, G.Q. Lu, X. Hu, Organophilicy of MCM-41 adsorbents studied by adsorption and temperature-programmed desorption, Colloids and Surface A: Physicochemical and Engineering Aspects 179 (2001) 261–269.
[7] N. Tanchoux, P. Trens, D. Maldonado, F.D. Renzo, F. Fajula, The adsorption of hexane over MCM-41 type materials, Colloids and Surface A: Physicochemical and Engineering Aspects 246 (2004) 1–8.
[8] J. Choma, S. Pikus, M. Jaroniec, Adsorption characterization of surfactant-templated ordered mesoporous silica synthesized with and without hydrothermal treatment, Applied Surface Science 252 (2005) 562–569.
[9] A.S. Araújo, M.J.B. Souza, A.O.S. Silva, A.M.G. Pedrosa, J.M.F.B. Aquino, A.C.S.L.S. Coutinho, Study of the adsorption properties of MCM-41 molecular sieves prepared at different synthesis times, Adsorption 11 (2005) 181–186.
[10] J.C. Vartuli, A. Malek, W.J. Roth, C.T. Kresge, S.B. McCullen, The sorption properties of as-synthesized and calcined MCM-41 and MCM-48, Microporous and Mesoporous Materials 44–45 (2001) 691–695.
[11] A.J. O'Connor, A. Hokura, J.M. Kisler, S. Shimazu, G.W. Stevens, Y. Komatsu, Amino acid adsorption onto mesoporous silica molecular sieves, Separation and Purification Technology 48 (2) (2006) 197–201.
[12] M. Ghiaci, A. Abbaspur, R. Kia, F. Seyedeyn-Azad, Equilibrium isotherm studies for the sorption of benzene, toluene, and phenol onto organo-zeolites and as-synthesized MCM-41, Separation and Purification Technology 40 (3) (2004) 217–229.
[13] M. Ghiaci, R. Kia, A. Abbaspur, F. Seyedeyn-Azad, Adsorption of chromate by surfactant-modified zeolites and MCM-41 molecular sieve, Separation and Purification Technology 40 (3) (2004) 285–295.
[14] X.S. Zhao, Q. Ma, G.Q. Lu, VOC removal: comparison of MCM-41 with hydrophobic zeolites and activated carbon, Energy & Fuels 12 (1998) 1051–1054.
[15] Y. Lu, H. Fan, A. Stump, T.L. Ward, T. Rieker, C.J. Brinker, Aerosol-assisted self-assembly of mesostructured spherical nanoparticles, Nature 398 (1999) 223.
[16] N. Baccile, D. Grosso, C. Sanchez, Aerosol generated mesoporous silica particles, Journal of Materials Chemistry 13 (2003) 3011–3016.
[17] Y.C. Lin, H. Bai, C.L. Chang, Applying hexagonal nanostructured zeolite particles for acetone removal, Journal of Air & Waste Management Association 55 (2005) 834–840.
[18] Y.C. Lin, H. Bai, Temperature effect on pore structure of nanostructured zeolite particles synthesized by aerosol spray method, Aerosol and Air Quality Research 6 (2006) 42–53.
[19] C.T. Hung, H. Bai, Adsorption behaviors of organic vapors using mesoporous silica particles made by evaporation induced self-assembly method, Chemical Engineering Science 63 (7) (2008) 1997–2005.
[20] H.Y. Fan, F. Van Swol, Y.F. Lu, C.J. Brinker, Multiphased assembly of nanoporous silica particles, Journal of Non-Crystalline Solids 285 (2001) 71–78.
[21] M.T. Bore, S.B. Rathod, T.L. Ward, A.K. Datye, Hexagonal mesostructure in powders produced by evaporation-induced self-assembly of aerosols from aqueous tetraethoxysilane solutions, Langmuir 19 (2003) 256–264.
[22] American Society of Testing Materials, Test method for measuring bulk density values of powders and other bulk solids, ASTM D6683-01, 2005.

[23] T.M. Wu, G.R. Wu, H.M. Kao, J.L. Wang, Using mesoporous silica MCM-41 for in-line enrichment of atmospheric volatile organic compounds, Journal of Chromatography A 1105 (2006) 168–175.
[24] F.T. Chang, Y.C. Lin, H.L. Bai, B.S. Pei, Adsorption and desorption characteristics of semiconductor volatile organic compounds on the thermal swing honeycomb zeolite concentrator, Journal of Air & Waste Management Association 53 (2003) 1384–1390.
[25] M. Lacroix, P. Nguyen, D. Schweich, C.P. Huu, S. Savin-Poncet, D. Edouard, Pressure drop measurements and modeling on SiC foams, Chemical Engineering Science 62 (2007) 3259–3267.